Liquid crystal ordering of DNA and RNA oligomers with partially overlapping sequences

2008 J. Phys.: Condens. Matter 20 494214

(http://iopscience.iop.org/0953-8984/20/49/494214)

J. Phys.: Condens. Matter **20** (2008) 494214 (6pp) doi:10.1088/0953-8984/20/49/494214

Liquid crystal ordering of DNA and RNA oligomers with partially overlapping sequences

G Zanchetta[1], M Nakata[2,3], M Buscaglia[1], N A Clark[2,4] and T Bellini[1,4]

[1] Dipartimento di Chimica, Biochimica e Biotecnologie per la Medicina, Università di Milano, Milano, Italy
[2] Department of Physics and Liquid Crystal Materials Research Center, University of Colorado, Boulder, CO 80309-0390, USA

E-mail: noel.clark@colorado.edu and tommaso.bellini@unimi.it

Received 14 August 2008
Published 12 November 2008
Online at stacks.iop.org/JPhysCM/20/494214

Abstract

We have recently shown that solutions of very short double-stranded B-DNA and A-RNA, down to six base pairs in length, can self-organize into chiral nematic and columnar liquid crystal (LC) phases. These observations were made on fully complementary sequences forming duplexes with blunt ends, where the LC ordering is due to base stacking forces promoting end-to-end aggregation of duplexes into living-polymer-type structures. Here we report LC formation in solutions of DNA and RNA 14mers forming double helices having single-stranded dangling ends that are 'sticky', i.e., mutually complementary with similar ends on other duplexes. This finding widens the conditions for spontaneous long range ordering in oligomeric nucleic acids, thus strengthening the notion that nucleic acids have remarkable self-assembly capability. Quantitative analysis of the phase diagram enables the extraction, within a nearest-neighbor interaction approximation, of the free energy associated with the pairing and stacking of nucleobases.

(Some figures in this article are in colour only in the electronic version)

1. Introduction

The richness and variety of the self-organization motifs of biomolecules are interesting, both because they often spring from subtle and marvelous combinations of many competing processes, and because understanding them is essential to an understanding of the origin and basic functioning of life. The self-organization of DNA has been extensively studied: since the early days of the deciphering of its double helix structure, DNA was known to exhibit gel-like phases that could be orientationally ordered, as perhaps best illustrated by the famous diffractogram Photo 51, taken by Rosalind Franklin on a sample made by pulling hydrated DNA fibers out of a concentrated solution. In those filamentous threads, DNA was in a columnar liquid crystal state, with the helices parallel to each other, but free to translate. The resulting lack of inter-chain positional periodicity, which initially made Photo 51 appear to be 'too simple' to be useful, left in the diffractogram only the information necessary to deduce the correct single molecule structure. Subsequent waves of interest into the phase behavior of DNA solutions have led to the recognition of its basic forms of liquid crystal (LC) ordering [1, 2], to the determination of phases behavior in a variety of conditions [3–5], and to the study of inter-helical interactions [6, 7]. DNA LC self-organization has also been studied in other contexts, related to its coiling into toroidal structures upon condensation [8], to its participation in the formation of highly structured complexes with cationic micelles [9], and to its intriguing *in vivo* structuring in bacteria highly resistant to adverse conditions [10, 11].

All these forms of ordering and self-assembly are observed in solutions of long DNA molecules with more than 100 base pairs (bp) and can be interpreted on the basis

[3] Deceased.
[4] Authors to whom any correspondence should be addressed.

of their elongated shape, their partial flexibility, their acidic nature, and their helical structure. Of key importance in this respect is the Onsager argument based on the evaluation of the translational and orientational entropy of rigid cylindrical particles having length L and diameter d [12]. According to this argument, at volume fractions above a critical value $\phi_c \sim 4d/L$, the tradeoff of orientational and translational entropy favors orientational ordering of the cylinders, provided that $L > 4d$. No ordering is expected in sub-Onsager regime ($L < 4d$). We have recently presented evidence that solutions of very short B-DNA double strands, 'nanoDNA', 6-20 bp in length, as well as of analogously short nanoRNA double strands, display liquid crystalline order [13, 14]. Despite the fact that the chiral nematic (N*) and the columnar (COL) phases observed in these solutions are of the same type as those observed in long DNA double strands, the interpretation cannot be just the same, since for these short strands $L < 3d$ and thus the oligomeric duplexes are not anisotropic enough in shape to satisfy the Onsager criterion. The phase behavior of nucleic acid oligomers is actually more intimately related to the mechanisms granting the double helix stability: the well known Watson–Crick base pairing and the less famous but equally important base stacking. Paired nucleobases are planar polycyclic aromatic hydrocarbons (PAHs) and thus are hydrophobic. In aqueous solution the bases stack to avoid exposure to water, leading to an attractive interaction that acts to hold them together when their flat aromatic faces are in contact [15]. This leads to the suggestion that the DNA duplex is a kind of chromonic LC, the LC family in which PAH dyes stack to form aggregates [16]. LC ordering of nanoDNA and nanoRNA appears to be a manifestation of the stacking forces acting between the paired terminal bases of different oligomeric duplexes [13]. These forces induce reversible linear aggregation of the oligonucleotides into effectively long chains, a process somewhat analogous to the 'living polymerization' of surfactants into rod-like micelles. When the physically bound, but chemically segmented, chains have an axial ratio and concentration large enough to enter the Onsager regime, the solution orders into the N* phase, and, upon further increasing the concentration, into the COL phase. The study of the N* and COL phase boundary hence provides a new direct route to evaluate the strength and the temperature dependence of the stacking forces.

Various models of linear reversible aggregation are available in literature [17–20]. They enable extracting the binding energy within the aggregate, from mean aggregation number, temperature and concentration of monomers. By adopting the simplified model in [19], in previous work we obtained an estimate of the end-to-end stacking free energy at 20 °C of $\delta G \sim 3$ kcal mol^{-1} and $\delta G \sim 4$ kcal mol^{-1} for blunt-ended DNA [13] and RNA [14], respectively. The case of nanoRNA is of particular interest for the present paper, since the RNA double helix unbinding temperature (T_U) is larger than that of DNA [21]. As a consequence, in the case of nanoRNA, T_U is about 30 °C larger than T_m, the clearing T of the LC phases. This gap has enabled us to determine T_m and, as a consequence, to estimate $d\delta G/dT$. Such an estimate was not possible in nanoDNA since in that case $T_U \sim T_m$, indicating that the phase melting may be due to the melting of the duplexes.

Here we study the behavior of concentrated solutions of partially complementary sequences forming duplexes with dangling unpaired nucleotides chosen so to favor stickiness among helices, finding liquid crystalline structures. We demonstrate that liquid crystallization of oligomeric nucleic acids can take place on the basis of a more general mechanism than previously described, involving both base stacking and base pairing.

In our previous studies on DNA [13] and RNA [14], we found that addition of a single or double dangling Thymine nucleotide to the 5′ terminal of the self-complementary Drew-Dickerson dodecamer (DD12) disrupts the LC ordering. We interpreted this finding as evidence that the dangling terminals sterically reduce the possibility of end-to-end stacking of duplexes. A similar behavior was also found in semidilute DNA solutions [22], where capping of the terminals affects their attractive interactions. In the present study, we report the concentration–temperature phase behavior of DNA and RNA 14mers, obtained by adding the sequence CG or AT to one terminal of DD12 or to the analogous sequence for RNA. In this way, and differently from our previous studies, we obtain partially self-complementary sequences that, upon hybridizing, expose at the terminals dangling, 'sticky' nucleotides providing attractive interactions between the duplexes. Interestingly, such binding mechanism was found to act in physiological processes [23] and is being studied as an effective means of condensation and packaging of DNA strands for gene delivery [24]. Here, we show that by combining pairing and stacking, DD12-AT and DD12-CG self-organize to form the same phases as DD12.

From the observed phase boundaries we extract the end-to-end adhesion energy at 20 °C, and, in some cases, we can also estimate $d\delta G/dT$. These estimates are here compared with those obtained by using the algorithms and the relative parameters developed to compute the thermodynamic quantities relevant in the formation and stability of the double helix oligomers (T_U, free energy, entropy and enthalpy). Several versions of these computation approaches are available, based on different oligonucleotide databases [25, 26], and tuned for various purposes. However, since such approaches yield values for end-to-end adhesion quite different from each other, introducing new strategies to better quantify pairing and stacking is of wide interest. The analysis here presented indeed results in a new route to access inter-strand interactions and hence to study the overall helical stability.

Having so extended the set of conditions for the stability of nanoDNA LC phases, we strengthen the notion that the staged self-assembly observed in concentrated solutions of oligomeric nucleic acids (duplexing, end-to-end adhesion, LC phase formation and phase separation [27]) may have been instrumental in early life as a means of templating the linear polymer structure of life's information carriers, since in the presence of appropriate chemistry it would strongly promote the elongation of already complementary oligomers.

Table 1. Temperature and concentration phase boundaries for the DNA and RNA sequences here investigated. In the columns we report the concentration at the I–N* (c_{IN}) and at the N*–COL (c_{NC}) phase boundary at 20 °C, the volume fractions ϕ_{IN} and ϕ_{NC} obtained from the c values by considering the bare chemical volume of the duplexes, the clearing temperatures $T_{m,N}$ ($T_{m,COL}$) at which the N* (COL) phase disappears from the sample, the duplex unbinding temperatures $T_{U,N}$ ($T_{U,COL}$) for molecules at concentrations forming, at low T, the N* (COL) phase, the end-to-end adhesion free energy δG extracted from the phase boundaries and its temperature dependence $d\delta G/dT$ determined in samples where $T_{m,N} \ll T_{U,N}$.

Sequence	c_{IN} (mg ml^{-1})	c_{NC} (mg ml^{-1})	ϕ_{IN}	ϕ_{NC}	$T_{m,N}$ (°C)	$T_{m,COL}$ (°C)	$T_{U,N}$ (°C)	$T_{U,COL}$ (°C)	δG (kcal mol^{-1})	$d\delta G/dT$ (kcal mol^{-1} K^{-1})
DNA DD12	700	1050	0.39	0.58	38	65	50	68	3.1	—
DNA DD12-AT	720	1150	0.40	0.64	33	50	50	68	2.9	−0.14
DNA DD12-CG	520	1000	0.29	0.55	40	70	50	68	3.6	—
RNA DD12	830	1280	0.46	0.71	30	60	60	90	4.0	−0.17
RNA DD12-CG	550	1150	0.30	0.64	49	75	60	90	4.7	−0.09

2. Experiments and results

The experiments discussed here have been performed on the following sequences. DNA: DD12 (5′-CGCGAATTCGCG-3′), DD12-AT (5′-CGCGAATTCGCGAT-3′), DD12-CG (5′-CGCGCGAATTCGCG-3′), DD12-TT (5′-CGCGAATTCGC GTT-3′). RNA: DD12 (5′-CGCGAAUUCGCG-3′), DD12-CG (5′-CGCGCGAAUUCGCG-3′), DD12-UU (5′-CGCGAAUUC GCGUU-3′). Sequences have been purchased from Primm S.r.l. (Milano, Italy) and Bionexus (Oakland, CA).

Solutions were prepared by dissolving oligomers in pure water. DNA and RNA concentrations, measured locally as described below, were always larger than 300 mg ml^{-1}. This corresponds to a large concentration of counterions, always larger than 1 M. Tests executed on samples prepared with added monovalent or divalent salt enough to double the effective ionic strength, yielded phase behavior quite similar to the one with no added salt (data not shown).

Cells were prepared by loading the sample solution in between two glass slides separated by thin polymer film spacers (6–10 μm). The desired concentration of the sample was obtained by evaporation, and the cells were then sealed with epoxy glue or fluorinated oil. When needed, a concentration gradient was obtained by thermally cycling the sample before sealing.

The cells have been characterized by:

(1) observation and identification of textures in depolarized transmission light microscopy (DTLM) and determination of T_m by observing the clearing of the LC textures;
(2) measurement of the optical spectrum of reflected light in cells built by using high refractive index glasses (F2, Schott AG, Mainz, Germany; $n = 1.62$). The reflected spectrum is measured in optical microscopy by illuminating a reduced portion of the cell and shows the distinctive periodic pattern expected from interference. Analysis of the spectrum enables determining the local refractive index of the solution and in turn the local DNA/RNA concentration [13];
(3) measurement, in fluorescence microscopy, of the emission intensity of ethidium bromide, doped in concentration of 1 molecule per helix in the DNA/RNA solutions. These data enable determining T_U.

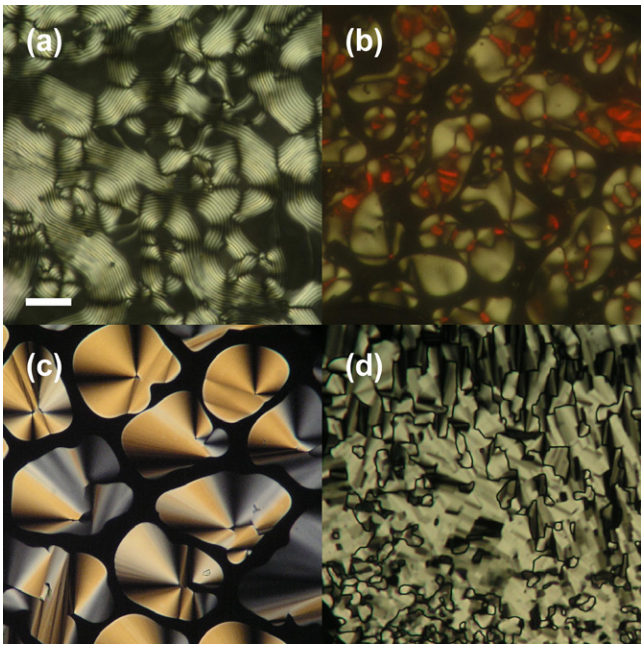

Figure 1. Polarized microscopy textures of LC phases of the investigated sequences. (a) Chiral nematic 'fingerprints' in a DNA DD12-CG sample. (b) Combined transmitted and reflected polarized microscopy image of the nematic phase of RNA DD12-CG. The red regions reveal a sub-micrometer pitch. (c) Developable domains of the columnar phase in a DNA DD12 sample. (d) Columnar phase of the DNA DD12-AT sequence. Size bar is 20 μm.

Except for DD12-TT and DD12-UU, in which the unpaired nucleotides impair end-to-end adhesion and hence LC phase formation, all other DNA and RNA samples organize in both the chiral nematic (N*) and the columnar (COL) phase depending on concentration and temperature, as shown in figure 1. By using the experimental procedures described above, we have characterized the phase diagram for all compounds, as reported in table 1, where we give the concentration of DNA/RNA at the I–N* (c_{IN}) and at the N*–COL (c_{NC}) phase boundary at 20 °C; the corresponding volume fractions ϕ_{IN} and ϕ_{NC} obtained by considering the bare chemical volume of the duplexes; the clearing temperatures $T_{m,N}$ ($T_{m,COL}$) at which the N* (COL) phase disappears from the sample, i.e. the upper limit of the T interval where the phase can be found; the duplex unbinding temperatures $T_{U,N}$

($T_{U,COL}$) measured at concentrations yielding N* (COL) phase at 20 °C. In table 1 we also indicate quantities resulting from data analysis as explained below.

Data in table 1 appear to be qualitatively coherent. In solutions of DNA DD12-AT the concentration needed for nematic ordering at 20 °C is larger than in the case of DD12, while the clearing temperature is lower. This behavior is consistent with what expected for a weaker end-to-end adhesion, providing shorter DNA aggregates and hence requiring a larger concentration to cross the Onsager line. This indicates that the presence of AT sticky ends slightly weakens the end-to-end adhesion energy with respect to the blunt end stacking of DD12. Different is instead the case of DNA DD12-CG, where the transition concentrations are quite smaller, indicating larger duplex adhesion energy. T_m are instead not very different, a behavior that can be understood by noticing that T_m are rather close to T_U, their difference being of the order of 10 °C, a T range comparable with the T spread of the duplex melting transition [14]. Thus, even if DNA DD12-CG forms more energetically stable living polymers than DNA DD12, their LC melting is limited by the unbinding of the helixes into single-stranded oligos, acting as contaminants and hence disrupting nanoDNA ordering. This analysis is confirmed by the RNA experiments. Concentration measurements also indicate that the CG sticky ends of RNA DD12-CG produce more stable end-to-end adhesion between duplexes than the stacking interaction between the blunt ends of RNA DD12. However in RNA the situation is different, since for RNA DD12, $T_m \ll T_U$. In this case, in fact, the addition of the CG terminals makes T_m significantly grow, while T_U remains the same. This condition enables extracting the T dependence of the duplex adhesion energy, as described in section 3.

3. Discussion

The finding of LC phases in the DNA DD12-AT and DD12-CG and in the RNA DD12-CG samples, and no ordering in the DNA DD12-TT and RNA DD12-UU samples, is a further clean indication that liquid crystallization of nanoDNA and nanoRNA proceeds from the end-to-end adhesion through the formation of linear aggregates, chemically discontinuous but physically bound 'living polymers'. When in a sample with a given DNA volume fraction ϕ, the average length $\langle L\rangle$ of the aggregates reaches the Onsager value $4d/\phi_c$, nematic ordering sets in [12, 19]. Since $\langle L\rangle$ depends on ϕ and on the adhesion energy δG, from the measured concentration we can extract δG, as previously done in studying DNA and RNA duplexes with no sticky dangling nucleotides. To do this we exploit the model by Cates, as reported in [19]

$$\langle L\rangle = \frac{N\ell}{2}\left(1+\sqrt{1+4\varphi e^{\varepsilon+k_I\varphi}}\right) \qquad (1)$$

where N is the number of nucleotides, ℓ is the rise along the helix axis relative to a single base pair (different in DNA and RNA), $\varepsilon \equiv \delta G/k_BT$ and $k_I \sim 1.45$ is a virial coefficient taking into account the steric repulsion between monomers. As done previously [13], in equation (1) the volume fraction ϕ is replaced by $\varphi = 0.5\phi/\phi_{NC}$, thus normalizing the concentration values over the value of ϕ_{NC}, which is generally expected, by a variety of theoretical approaches, to be $\phi_{NC} \sim 0.5$ [28–30]. In this simple way we take into account the effects of electrostatic repulsion between the duplexes: in fact, because of repulsion, DNA solutions generally behave as if the duplex diameter, and hence the DNA volume fraction, were larger [31] than what expected on the basis of their bare chemical volume. Such normalization scales this effect, on which we have no direct control, enabling comparing the experimental I–N* phase boundary with the Onsager line.

The values for δG obtained through this analysis are reported in table 1. We find that the pairing of CG sticky ends increases the end-to-end adhesion by 0.5–0.7 kcal mol^{-1} relative to DD12, while AT terminals decrease the adhesion of a smaller quantity.

As T is increased above 20 °C, the N* phase starts to melt, with the local melting temperature increasing with concentration. Therefore, the N* volume within the cell gradually shrinks. Upon increasing T, the last portion of N* turning isotropic, at $T_{m,N}$, is the one in contact with the COL phase region of the sample, hence having the largest concentration, i.e. c_{NC}. The melting process in a typical cell is described in figure 2. From c_{NC} and $T_{m,N}$ we extract the adhesion energy $\delta G(T_{m,N})$ with the same procedure used for the measurement at 20 °C. In this way we could extract the values of $d\delta G/dT$ reported in table 1.

The analysis of nanoDNA and nanoRNA LC phase diagram, enabling quantitative estimates of the binding energies, appears as a new route to the quantification of pairing and stacking forces in nucleic acids. While we postpone the definition of a complete set of the pairing combination to a future, more systematic investigation, here we discuss the relationship between our finding and the values expected on the basis of the database currently used to evaluate the binding energies of DNA double strands. Within the frame of such calculations, the free energy gain associated to the end-to-end adhesion through pairing of complementary dangling ends can be estimated considering the free energy difference between the two different situations (e.g. for the DD12-CG sequence) of (I) separate, unbound helices

5′-CGCGCGAATTCGCG-3′

3′-GCGCTTAAGCGCGC-5′

5′-CGCGCGAATTCGCG-3′

3′-GCGCTTAAGCGCGC-5′

and of (II) helices with paired dangling ends

5′-CGCGCGAATTCGCG/CG-CGCGAATTCGCG-3′

3′-GCGCTTAAGCGC-GC/GCGCTTAAGCGCGC-5′

where '-' indicates the phosphodiester bond and '/' indicates the coaxial stacking interaction between two facing bases without a covalent bond in the phosphate backbone, also known as nick. Accordingly, ΔG_I is the free energy difference between the two duplexes of state (I) and the four single strands components, while ΔG_{II} refers to the difference between the associated duplexes and the same four single strands. Here we are interested in the difference between the two, i.e. $\delta G = \Delta G_{II} - \Delta G_I$.

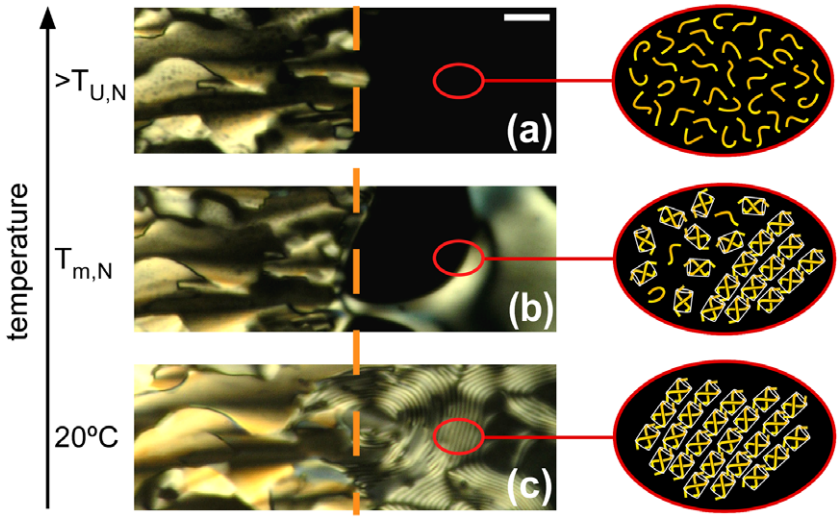

Figure 2. Temperature dependence of the N*–COL phase boundaries as observed in DTLM in a DNA DD12-CG sample. Within the pictures $c \sim c_{NC}$. At 20 °C (panel (c)) the COL and N* phase coexist (the orange dashed line approximately indicates the location of the interface). As T is increased to $T_{m,N}$, the N* phase melts first coexisting with the isotropic phase (panel (b)), to eventually turn into an isotropic phase of dispersed duplexes. As T is further increased to $T_{U,N}$ (panel (a)), the solutions transforms into an isotropic phase of single-stranded DNA. Size bar is 20 μm.

The pairing and stacking energy contributions within helices, on the basis of which to evaluate ΔG_{I} and ΔG_{II}, are calculated with the standard nearest-neighbor approximation [32] at 20 °C from the reported enthalpy and entropy parameters [26]. This is done by assuming an effective ionic strength of 1 M monovalent salt, the reference condition adopted to determine the database values [26]. The additional stabilizing effect of unpaired dangling ends to the free energy of the two separate DD12-CG duplexes is also taken into account [33]. As regards coaxial stacking energy, different values are found in literature [34–37], which yield rather different estimates of the total binding energy, within a factor of 2. We chose to use values from [34] since they were obtained within the same frame of the nearest-neighbor parameters. Accordingly, in the case of DD12-CG, $\delta G = \Delta G_{init} - 2\Delta G_{DE} + \Delta G_{CG/GC} + 2\Delta G_{coax} \sim 6.5$ kcal mol^{-1} at 20°, where ΔG_{init} is the entropic penalty to keep together the two duplexes, ΔG_{DE} is the stabilizing effect of dangling ends to the two separate duplexes in state (I), $\Delta G_{CG/GC}$ and ΔG_{coax} are the contributions to the stability of state (II) of the paired CG terminals and of the coaxial stacking at the two nicks. Analogous computation yields $\delta G \sim 4.2$ kcal mol^{-1} in the case of DD12-AT. Unfortunately, a similar approach does not allow us to calculate within the same frame the stacking energy of well-terminated duplexes, since a database for blunt ends stacking is not available and the use of coaxial stacking parameters would be arbitrary. From the analysis of the DNA database, it is also possible to extract the T dependence of the binding free energy for the two sequences with sticky ends here discussed. Since enthalpic contributions are basically independent on T, $\delta G/\mathrm{d}T$ corresponds to the sticky ends adhesion entropy. For DD12-CG and DD12-AT we find respectively $\delta G/\mathrm{d}T \sim -0.07$ kcal mol^{-1} and $\delta G/\mathrm{d}T \sim -0.12$ kcal mol^{-1}.

These evaluations are in satisfactory agreement with the data in table 1, the differences, of about a factor 1.5 or less, being smaller than the variation of the parameters extracted from the different databases. Our data confirm that CG sticky ends induce a stronger adhesion energy than AT and enable to compare the adhesion strength mediated by AT and CG sticky ends with the blunt end stacking of DD12. The fact that the AT adhesion has the same free energy than the blunt end adhesion confirms the end-to-end stacking as an interaction of relevant magnitude. CG pairing increases instead the end-to-end adhesion by 0.5 kcal mol^{-1} in both DNA and RNA. Furthermore, our data confirm that the stacking is stronger in RNA than in DNA, a concept that agrees with the larger temperature stability of RNA duplexes with respect to DNA duplexes (T_U in table 1). These results indicate that the analysis of the phase behavior is a new route to the quantitative study of DNA pairing and stacking energies.

The observation, here reported and discussed, that solutions of double strands with mutual partial overlap order into LC phases, contributes to the notion that LC packing of DNA may have an important biological relevance in the genome repair mechanisms of certain bacteria. Tight and ordered DNA packing has been proposed by A. Minsky and co-workers as a physical strategy to protect the genome of bacteria under prolonged environmental stress, such as starvation and intense radiation. Starved *Escherichia coli* cells show spontaneous DNA packing through a non-enzymatic and fully reversible phase transition [10]. In wild-type bacteria the process is optimized by the formation of micro-crystalline assemblies of DNA and Dps, a non-specific DNA binding protein, whose activity is regulated by the intracellular concentration of polyvalent cations. However, bacteria that lack Dps also show spontaneous DNA packing in starving conditions: in this case, the DNA undergoes a reversible transition into a chiral nematic phase, also found in slowly growing bacteria and in primitive algae [38, 39]. Bacteria with exceptionally high radio-resistance arrange their DNA in tightly bundled toroids under conspicuous irradiation [11].

Similar structures are also found in dormant spores and can be reproduce *in vitro* by exposing DNA to various packaging agents [40]. This general behavior appears to increase the survival to conditions where the probability of double-strand breaks is significant or, in general, exceeds the repair capability of the cell machinery, as in the case of starvation.

The ordered packing of the genome enables a form of non-templated DNA repair as long as the packing is resistant to multiple fractures on both DNA strands, and hence it implies the notion that the ordering is preserved even if the double helix is interrupted in both strands. Our results demonstrate that this is indeed the case, since the LC phases originally considered possible in solutions of long double-stranded DNA molecules have been found to persist both when both strands are interrupted at the same position [13] and when the two strands are cleaved in position shifted by 2 bases, all the larger shifts inducing a larger interactions and hence larger LC phase stability.

4. Conclusions

Two principal results derive from these experiments. First we have shown that the weak attractive interaction between duplexes due to the pairing of two dangling nucleobases at their terminals provides sufficient free energy to promote the formation of long range liquid crystalline ordering in solutions of oligomeric DNA and RNA. This adds on to the already observed supramolecular self-assembly capability in solutions of duplexes with blunt ends. The end-to-end adhesion of oligomeric duplexes promoted by a delicate combination of pairing and stacking may have been instrumental in promoting the initial prebiotic formation of linear polymers of nucleic acids.

Moreover, since the end-to-end adhesion studied here involves both base pairing and base stacking interactions, and may be compared to the base stacking-only situation of blunt end DNA, the phase diagrams presented offer a new route to quantify the free energy associated in the Watson–Crick pairing of two DNA or RNA strands into double helices. The quantitative analysis confirms—as expected—that CG/GC association is stronger than AT/TA, but also enables comparing CG/GC and AT/TA association with blunt end stacking, an assessment difficult to obtain with different procedures. We find that AT/TA pairing + stacking is quite similar, in strength, to the blunt end stacking. Further systematic study of phase diagrams of various sequences will enable to provide a new test bed for the conventional models commonly used to evaluate the interactions strength in nucleic acids oligomers.

Acknowledgments

N Peyret is kindly acknowledged for discussions and for providing the coaxial stacking data from his PhD thesis. This work was supported by US NSF Grants DMR 0820579 and DMR 0606528.

References

[1] Luzzati V and Nicolaieff V A 1959 *J. Mol. Biol.* **1** 127
[2] Robinson C 1961 *Tetrahedron* **13** 219
[3] Strzelecka T E, Davidson M W and Rill R L 1988 *Nature* **331** 457
[4] Livolant F, Levelut A M, Doucet J and Benoit J P 1989 *Nature* **339** 724
[5] Livolant F and Leforestier F A 1996 *Prog. Polym. Sci.* **21** 1115
[6] Podgornik R, Strey H H and Parsegian V A 1998 *Curr. Opin. Colloid Interface Sci.* **3** 534
[7] Kornyshev A A, Lee D J, Leikin S and Wynveen A 2007 *Rev. Mod. Phys.* **79** 943
[8] Hud N V and Downing K H 2001 *Proc. Natl Acad. Sci. USA* **98** 14925
[9] Safinya C R 2001 *Curr. Opin. Struct. Biol.* **11** 440
[10] Frenkiel-Krispin D, Levin-Zaidman S, Shimoni E, Wolf S G, Wachtel E G, Arad T, Finkel S E, Kolter R and Minsky A 2001 *EMBO J.* **20** 1184
[11] Levin-Zaidman S, Englander J, Shimoni E, Sharma A K, Minton K W and Minsky A 2003 *Science* **299** 254
[12] Onsager L 1949 *Ann. New York Acad. Sci.* **51** 627
[13] Nakata M, Zanchetta G, Chapman B D, Jones C D, Cross J O, Pindak R, Bellini T and Clark N A 2007 *Science* **318** 1276
[14] Zanchetta G, Bellini T, Nakata M and Clark N A 2008 *J. Am. Chem. Soc.* **130** 12864
[15] Calladine C R, Drew H R, Luisi B F and Travers A A 2004 *Understanding DNA: The Molecule and How it Works* 3rd edn (San Diego, CA: Elsevier–Academic)
[16] Lydon J 2004 *J. Colloid Interface Sci.* **8** 480
[17] Cates M E and Candau S J 1990 *J. Phys.: Condens. Matter* **2** 6869
[18] Horowitz V R, Janowitz L A, Modic A L, Heiney P A and Collings P J 2005 *Phys. Rev.* E **72** 041710
[19] Lü X and Kindt J T 2004 *J. Chem. Phys.* **120** 10328
[20] Sciortino F, Bianchi E, Douglas J F and Tartaglia P 2007 *J. Chem. Phys.* **126** 194903
[21] Wang S and Kool E T 1995 *Biochemistry* **34** 4125
[22] Li L, Pabit S A, Lamb J S, Park H Y and Pollack L 2008 *Appl. Phys. Lett.* **92** 223901
[23] Qiu H, Dewan J C and Seeman N C 1997 *J. Mol. Biol.* **267** 881
[24] Sarkar T, Conwell C C, Harvey L C, Santai C T and Hud N V 2005 *Nucleic Acids Res.* **33** 143
[25] Breslauer K J, Frank R, Blöcker H and Marky L A 1986 *Proc. Natl Acad. Sci. USA* **83** 3746
[26] Santalucia J 1998 *Proc. Natl Acad. Sci. USA* **95** 1460
[27] Zanchetta G, Nakata M, Buscaglia M, Bellini T and Clark N A 2008 *Proc. Natl Acad. Sci. USA* **105** 1111
[28] Taylor M P and Herzfeld J 1990 *Langmuir* **6** 911
[29] Bates M A and Frenkel D 1998 *J. Chem. Phys.* **109** 6193
[30] Bohle A M, Holyst R and Vilgis T 1996 *Phys. Rev. Lett.* **76** 1396
[31] Merchant K and Rill R L 1997 *Biophys. J.* **73** 3154
[32] SantaLucia J and Hicks D 2004 *Annu. Rev. Biophys. Biomol. Struct.* **33** 415
[33] Bommarito S, Peyret N and SantaLucia J 2000 *Nucleic Acids Res.* **28** 1929
[34] Peyret N 2000 *PhD Thesis* Wayne State University
[35] Protozanova E, Yakovchuk P and Frank-Kamenetskii M D 2004 *J. Mol. Biol.* **342** 775
[36] Vasiliskov V A, Prokopenko D V and Mirzabekov A D 2001 *Nucleic Acids Res.* **29** 2303
[37] Pyshnyi D V and Ivanova E M 2002 *Russ. Chem. Bull. Int Edn* **51** 1145
[38] Livolant F 1991 *Physica* A **176** 117
[39] Leforestier A and Livolant F 1993 *Biophys. J.* **65** 56
[40] Minsky A 2003 *Mol. Microbiol.* **50** 367